Investigation of low-spin states in ^{92}Zr with the $(n,n'\gamma)$ reaction

C. Fransen,[1,2] V. Werner,[2,*] D. Bandyopadhyay,[1] N. Boukharouba,[1] S. R. Lesher,[1,†] M. T. McEllistrem,[1] J. Jolie,[2] N. Pietralla,[2,3] P. von Brentano,[2] and S. W. Yates[1]

[1]*Departments of Physics & Astronomy and Chemistry, University of Kentucky, Lexington, Kentucky 40506-0055*

[2]*Institut für Kernphysik, Universität zu Köln, D-50937 Köln, Germany*

[3]*Department of Physics & Astronomy, State University of New York, Stony Brook, New York 11794-3800*

(Received 16 November 2004; published 12 May 2005)

Excited low-spin states of ^{92}Zr have been studied with the $(n,n'\gamma)$ reaction. Comprehensive data on the electromagnetic decay of states with excitation energies up to about 3.8 MeV in particular, lifetimes, γ-ray branching ratios, multipole mixing ratios, and absolute transition strengths have been obtained. The detailed spectroscopic information about the low-spin level scheme enables us to address the predominant proton-neutron symmetry for low-spin states of ^{92}Zr. These data are compared to those of corresponding states in the $N = 52$ isotone ^{94}Mo and to a shell model calculation using ^{88}Sr as an inert core. However, neither a purely collective picture nor the restricted shell model calculation yields a fully satisfactory description of the observed structures.

DOI: 10.1103/PhysRevC.71.054304 PACS number(s): 21.10.Re, 21.10.Tg, 25.40.Fq, 27.60.+j

I. INTRODUCTION

The nuclide $^{92}_{40}Zr_{52}$ belongs to the $N = 52$ isotones for which evidence for proton-neutron mixed-symmetry multiphonon structures of vibrational nature was recently observed [1–7]. With 52 neutrons, ^{92}Zr has only two valence neutrons outside the $N = 50$ shell closure; however, the situation for the protons is more complicated. From the shell model, one expects a proton subshell closure for the zirconium isotopes with the $\pi(2p_{1/2})$ proton orbital fully occupied. Indeed, lower $E2$ collectivity is found in ^{92}Zr than in the heavier $N = 52$ isotones, ^{94}Mo and ^{96}Ru, where excited states with clear characteristics of collective multiphonon excitations were identified from absolute transition strengths [1–6]. A study of the neighboring ^{94}Mo in the shell model [8] permitted, however, a successful description of the low-spin level scheme of that nucleus only with an $^{88}_{38}$Sr core, thus taking into account important configurations with holes in the $\pi(2p_{1/2})$ orbital. This result has (model dependently) demonstrated the breaking of the ^{90}Zr core for the proton configurations. A direct measurement of observables requiring active proton configurations in a Zr isotope could sensitively test the shell model. Nuclear g factors of low-spin states or of proton-neutron mixed-symmetry states and their properties represent such observables [7,9].

In recent studies of ^{94}Mo [1–4], and ^{96}Ru [5,6], both proton-neutron (pn) symmetric and isovector excitations were found. The latter are called mixed-symmetry (MS) states because they are neither fully symmetric nor fully antisymmetric with respect to the pn degree of freedom. These states are of considerable interest since they are particularly sensitive to the pn interaction, and they are predicted in the pn version of the interacting boson model (IBM–2) [10–13].

In the recently proposed Q-phonon scheme [14–17], which is an approximate scheme in the IBM, the lowest pn symmetric and MS states can be approximated by simple expressions with the proton and neutron quadrupole operators Q_p and Q_n. The pn symmetric Q-phonon Q_s results from a symmetric coupling of these quadrupole excitations of the valence protons and neutrons $Q_s = \mathcal{N}(Q_p + Q_n)$, the MS Q-phonon $Q_{\rm ms}$ from a partially antisymmetric coupling $Q_{\rm ms} = \alpha Q_p - \beta Q_n$ [1].

In vibratorlike nuclei, the existence of a fundamental one-phonon 2^+ MS state ($2^+_{1,\rm ms}$) with the structure $|2^+_{1,\rm ms}\rangle = Q_{\rm ms}|0^+_1\rangle$ is expected. This state is similar to the 2^+_1 state in these nuclei, which represents a pn symmetric one-quadrupole phonon excitation with the structure $|2^+_1\rangle = Q_s|0^+_1\rangle$. These pn symmetric and nonsymmetric one-phonon states act in the IBM–2 as building blocks of nuclear structure and are able to form multiphonon states, e.g., a multiplet of two-phonon MS states with the structure

$$|L^\pi\rangle \propto (Q_s Q_{\rm ms})^{(L)}\left|0^+_1\right\rangle \quad \text{with} \quad L = 0,\ldots,4. \tag{1}$$

A systematic description of MS states in the IBM together with predictions of their properties can be found in Ref. [18].

In $^{94}Mo_{52}$, the fundamental $2^+_{1,\rm ms}$ and the 1^+, 2^+, and 3^+ members of the aforementioned two-phonon multiplet of MS states with the structure $(2^+_1 \otimes 2^+_{1,\rm ms})$ were clearly identified [1–4]. In neighboring $^{96}Ru_{52}$, the $2^+_{1,\rm ms}$ state was found [5,6], and candidates for two-phonon MS states were assigned from $E2/M1$ mixing ratios, branching ratios, and lifetime limits [6].

In vibrational nuclei, signatures of MS states, accessible through γ-ray spectroscopy at rather low excitation energies, are strong $M1$ transitions to symmetric states with the same phonon number with matrix elements of about $|\langle J^f_{\rm sym}\|M1\|J^i_{\rm ms}\rangle| \approx 1\mu_N$, and weakly collective $E2$ transitions to symmetric states, since the latter transitions stem from the annihilation of a MS phonon $Q_{\rm ms}$. In contrast, we expect collective $E2$ transitions with transition strengths of several Weisskopf units between states with the same proton-neutron symmetry, e.g., from the MS two-phonon states to the $2^+_{1,\rm ms}$ state from the annihilation of a symmetric phonon Q_s.

*Present address: Wright Nuclear Structure Laboratory, Yale University, New Haven, Connecticut 06520-8124.

†Present address: Instituut voor Kern- en Stralingsfysica, Katholieke Universiteit Leuven, 3001 Leuven, Belgium.

The goal of this work was to investigate the evolution of collectivity and proton-neutron symmetry in a transition from semiclosed shell nuclei with shell model structure, arising from subshell closures at $Z = 38$ and $Z = 40$, to more collective nuclei and, in particular, the impact of the single-particle effects on the formation of MS states. The results of our measurements on ^{92}Zr give information about the shell structure in this mass region. Level energies, lifetimes, decay branching ratios, and multipole mixing ratios were measured to determine the level scheme of ^{92}Zr, and absolute transition strengths allowed the interpretation of excited states. To date, lifetime information for ^{92}Zr has been rather sparse with only a few lifetimes in the picosecond range known [19]. In addition, lifetimes and parities of some $J = 1$ and $J = 2$ states were measured in recent photon scattering experiments [7,20]. For our study of ^{92}Zr, we used the method of inelastic neutron scattering, $(n,n'\gamma)$, which allows a comprehensive study of excited low-spin states in the sense that all low-spin states in the investigated energy range are populated by this reaction, regardless of their structure. The experiments were performed at the neutron scattering facility at the University of Kentucky.

In Sec. II, the experimental methods are briefly described, and Sec. III contains a more detailed discussion of some excited states of ^{92}Zr. Section IV gives a comparison to corresponding data in the neighboring nucleus ^{94}Mo and an interpretation in terms of the spherical shell model.

II. EXPERIMENTAL METHOD, DATA EVALUATION

Experiments with the $(n,n'\gamma)$ reaction on ^{92}Zr were performed by Glasgow and coworkers [21] in the late 1970s. The level scheme was investigated in these experiments up to an energy of about 3.5 MeV, and neutron scattering cross sections were determined. Since level lifetimes were not measured, no information about transition strengths was available from their data.

Our measurements on ^{92}Zr were performed using the $(n,n'\gamma)$ reaction with the neutron scattering setup of the 7 MV electrostatic accelerator at the University of Kentucky [22]. As a neutron source, the ^{3}H$(p,n)^3$He reaction was used. Protons passed through an 8-μm thick molybdenum foil into a gas cell 30 mm in length and 10 mm in diameter containing ^{3}H at a pressure of nearly 1 atm. The average current of the proton beam was 2 μA, and the energy spread of the neutrons at the sample position was about 60 keV. The proton beam was pulsed at 1.875 MHz with a pulse width of about 10 ns, then bunched to a 1 ns width. The massive 41.1415 g metallic cylindrical Zr sample with a diameter of 2 cm and a length of 2 cm was enriched in ^{92}Zr to 95.16%. It was suspended in the neutron flux at a distance of about 60 mm from the end of the gas cell.

γ rays were detected with a Compton-suppressed HPGe detector with an efficiency of 55% relative to a 7.6 × 7.6 cm NaI detector. The HPGe detector and the BGO annulus were shielded against the neutrons and background radiation with boron-loaded polyethylene, copper, and tungsten. The distance of the HPGe detector from the center of the sample was about 1.1 m. To monitor the neutron flux incident upon the ^{92}Zr sample, we placed a Hansen-McKibben long counter

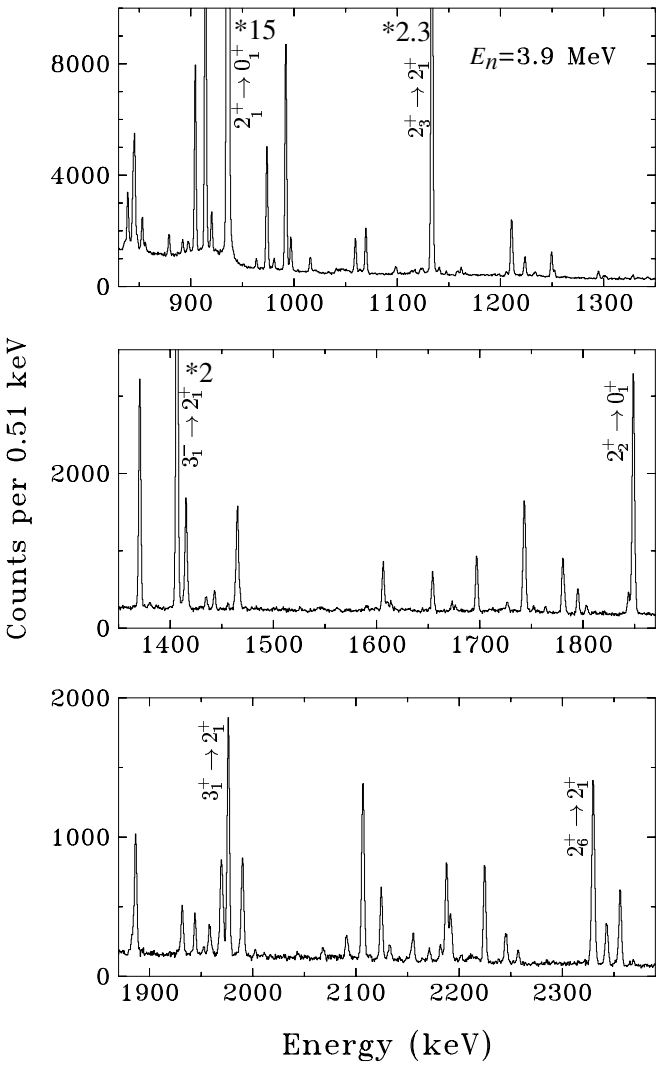

FIG. 1. γ-ray spectrum in the energy range from 830 to 2400 keV from the ^{92}Zr$(n,n'\gamma)$ reaction at an incident neutron energy of 3.9 MeV. Some intense transitions in ^{92}Zr are labeled. The additional labels, such as "*2", depict the fraction of the corresponding γ-ray line that is not displayed in the spectrum.

at 90 degrees relative to the axis of the incident beam at approximately 4 m from the sample. Time-of-flight techniques were used to discriminate between the prompt γ rays from the $(n,n'\gamma)$ reaction in the sample, background γ rays, and γ rays from neutron scattering reactions in the spectrometer, e.g., in the Ge crystal of the HPGe detector itself. Figure 1 shows a typical γ-ray spectrum from the ^{92}Zr$(n,n'\gamma)$ reaction. Further details about the neutron scattering facility, the time-of-flight measurements, neutron monitoring for normalization, and data reduction techniques have been described in Refs. [22,23].

γ-ray angular distribution measurements were performed on ^{92}Zr with neutron energies of $E_n = 2.2$ and 3.9 MeV. In the experiment at $E_n = 3.9$ MeV, the γ radiation from the target was measured at 12 angles from 40 to 150 degrees relative to the beam axis. γ-ray spectra were measured for 12 hours at each angle. The second angular distribution measurement with $E_n = 2.2$ MeV served primarily for the

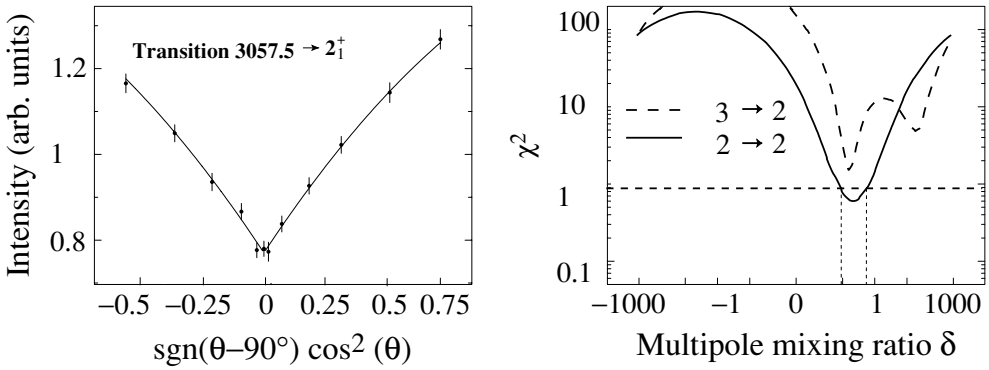

FIG. 2. Determination of the spin of the 3057.5-keV level and the multipolarity of the decay transition to the 2_1^+ state from the $(n,n'\gamma)$ angular distribution measurement. The left panel shows the angular distribution of the 2123.0-keV transition to the 2_1^+ state, including the best fit to an even-order Legendre polynomial with the parameters A_0, A_2, and A_4. The right panel depicts χ^2 for this fit versus the $E2/M1$ mixing ratio δ for initial spins of $J = 2$ and 3. $J = 2$ yielded the best fit. Due to the strong ground-state decay, spin $J = 3$ and negative parity can be excluded for the 3057.5-keV level. The data yield a mixing ratio for the decay to the 2_1^+ state of $\delta = 0.69(16)$, also ruling out negative parity.

determination of the lifetimes of the 2_2^+ and 2_3^+ states, without sidefeeding from higher lying excited states. The emitted γ rays were measured at eight different angles for 4 hours each. From these experiments, we determined spins of excited states and multipolarities of decay transitions by fitting the experimentally determined angular distributions of the emitted γ rays with even-order Legendre polynomial expansions and comparing them to theoretical calculations performed with a modified form of the statistical model program code CINDY [24].

Figure 2 shows data from which the spin assignment for the 3057.5-keV level and the multipole mixing ratio of the decay transition to the 2_1^+ state were determined. The left portion of Fig. 2 depicts the normalized experimental γ-ray intensities of the decay transition to the 2_1^+ state versus the γ-ray emission angle relative to the incident beam axis and the fit to even-order Legendre polynomials. The right part shows χ^2 for this fit versus the multipole mixing ratio δ. The spin assignment $J = 2$ for the 3057.5-keV level and an $E2/M1$ mixing ratio of $\delta = 0.69(16)$ give the best fit. In addition, a spin of 3 can be excluded because of the rather strong decay of the 3057.5-keV level to the ground state.

We obtained lifetimes with the Doppler-shift attenuation method (DSAM). The γ-ray peaks have centroids with the angular dependence given by

$$E_\gamma(\theta) = E_0\left(1 + F(\tau)\frac{v_{\rm cm}}{c}\right)\cos(\theta), \qquad (2)$$

where E_0 is the unshifted γ-ray energy, θ is the emission angle relative to the incident beam, $E_\gamma(\theta)$ is the centroid energy of a γ-ray peak at the angle θ, and $F(\tau)$ is the Doppler-shift attenuation factor. The theoretical $F(\tau)$ values were calculated using the theory of Winterbon [25] with slight modifications as described in Ref. [26]. The maximum recoil velocity was $v_{\rm cm} = 9.8 \cdot 10^{-4}c$ for an incident neutron energy of $E_n = 3.9$ MeV. As energy normalization standards, a ^{137}Cs source with a γ ray at 661.660(3) keV [27] and a ^{24}Na source with γ rays at 1368.633(6) and 2754.030(14) keV [28] were measured simultaneously. The ^{24}Na source was only used for 4 hours of every 12-hour run for each angle in the experiment with $E_n = 3.9$ MeV, because its 1368.6-keV γ ray is nearly the same as a γ ray from ^{92}Zr.

The clearly observable Doppler shifts of many γ rays from short-lived states allowed determinations of lifetimes in the range from a few femtoseconds to about one picosecond. The uncertainties of the lifetimes given in Table I result from both the statistical errors and the uncertainties in the stopping powers, which we assume to be about 10%.

Figure 3 depicts the lifetime determinations of the 2_2^+ state from the Doppler shift of the $2_2^+ \rightarrow 2_1^+$ transition at 912.8 keV in the experiment with $E_n = 2.2$ MeV and of the 1_2^+ state at 3472.1 keV from the Doppler shift of the ground-state transition in the measurement with $E_n = 3.9$ MeV. Note that the Doppler-shifted energies of the 3472.1-keV transition at the extreme angles differ by about 5 keV.

An excitation function measurement was performed with neutron energies from 2.6 to 3.9 MeV by increasing the energy in 100-keV steps. At each energy, the spectrum was accumulated for about 8 hours. From this experiment, we obtained considerable information about the level scheme of ^{92}Zr; in particular, the data allowed unique placements of newly observed decay transitions into the level scheme. In addition, spin assignments from the angular distribution measurements were verified by comparing the experimental neutron scattering cross sections to the results of calculations with the code CINDY [24]. The neutron scattering cross sections are dependent on the energy of the incident neutrons and the spins of the excited states. Therefore, these cross sections yield information about the spins of excited states. Figure 4 displays the experimental data and the results of a calculation with the code CINDY for the 3262.9-keV level for the spin hypotheses $J = 0-4$ as an example. As can be seen from Fig. 4, spins of $J = 0$, 1, and 4 can be clearly excluded for the 3262.9-keV level. Good agreement with the experimental data was found both for $J = 2$ and $J = 3$, but $J = 3$ is ruled out by the fast ground-state transition. In addition, a recent investigation of ^{92}Zr with inelastic photon scattering clearly resulted in the assignment of $J = 2$ for this state [7].

TABLE I. Experimental results from the ^{92}Zr$(n,n'\gamma)$ experiments performed at the neutron scattering facility of the University of Kentucky. The table contains the level and transition energies, the spins of the corresponding states, relative intensities I_γ, multipole mixing ratios δ, lifetimes τ, and Doppler-shift attenuation factors $F(\tau)$. Lifetimes marked with a superscript "a" were taken from [19]. "n" in the first column marks excited states observed in the ^{92}Zr$(n,n'\gamma)$ experiments for the first time; "n" in the fourth column marks transitions observed for the first time. "n" in the second column shows new or better spin assignments than are given in [19]. If two values for the multipole mixing ratio δ are given, the determination was ambiguous.

E_x (keV)	J_i^π	J_f^π	E_γ (keV)	I_γ (%)	δ	τ (fs)	$F(\tau)$
934.46(10)	2_1^+	0_1^+	934.5(1)	100.0	0	7210(580)[a]	–
1382.8(1)	0_2^+	2_1^+	448.3(1)	100.0	0	127(4) ps[a]	–
1495.5(1)	4_1^+	2_1^+	561.1(1)	100.0	0.04(2)	147(4) ps[a]	–
1847.3(1)	2_2^+	0_1^+	1847.2(1)	44.6(23)	0	138(14)	0.249(4)
		2_1^+	912.8(1)	100.0(23)	−0.04(2)		
2066.6(1)	2_3^+	0_1^+	n 2066.7(4)	0.528(67)	0	>1100	0.029(10)
		2_1^+	1132.1(1)	100.0(50)	$-3.2^{+0.5}_{-0.4}$		
		2_2^+	219.3(2)	0.61(12)	–		
2339.6(1)	3_1^-	2_1^+	1405.1(1)	100.0(50)	0.03(2)	407(43)	0.108(4)
		4_1^+	844.1(2)	32.3(18)	–		
		2_2^+	492.4(3)	11.69(65)	0.01(3)		
2398.4(1)	4_2^+	2_1^+	1463.8(2)	35.9(23)	$-0.13^{+0.05}_{-0.06}$	215(23)	0.193(5)
		4_1^+	902.9(1)	100.0(23)	$-0.11^{+0.03}_{-0.02}$		
2485.9(2)	5_1^-	4_1^+	990.5(2)	100.0	doublet	–	–
2743.5(2)	$(4)^-$	4_1^+	1248.0(3)	100.0(54)	$0.02^{+0.06}_{-0.04}$	>3800	0.003(10)
		3_1^-	403.9(2)	56.6(34)	0.04(2)		
		5_1^-	257.6(2)	90.1(50)	$-0.01^{+0.02}_{-0.03}$		
2819.6(1)	2_4^+	0_1^+	2819.3(7)	4.53(40)	0	92(10)	0.365(6)
		2_1^+	1885.0(2)	34.2(19)	$3.7^{+0.7}_{-0.5}$ −0.14(4)		
		2_2^+	972.3(1)	100.0(51)	0.01(2) $(2.3^{+0.2}_{-0.1})$		
2864.7(2)	4_3^+	2_1^+	1930.2(3)	26.7(17)	−0.02(4)	339^{+43}_{-40}	0.125(8)
		4_1^+	1369.2(2)	100.0(52)	−0.49(5)		
		4_2^+	n 466.4(3)	11.1(10)	$-0.01^{+0.15}_{-0.13}$		
2904.0(2)	0_3^+	2_1^+	1969.6(3)	43.7(54)	0	1200^{+820}_{-340}	0.043(18)
		2_3^+	837.4(2)	100.0(54)	–		
2909.3(2)	3_1^+ n	2_1^+	1974.8(2)	100.0(51)	–	311(35)	0.127(6)
		4_1^+	1413.8(4)	78.3(40)	$-0.50^{+0.06}_{-0.07}$ $-1.49^{+0.16}_{-0.14}$		
		2_3^+	842.7(4)	46.2(33)	$-0.25^{+0.07}_{-0.09}$		
3039.8(3)	3 n	2_1^+	2105.2(3)	100.0(18)	$0.02^{+0.03}_{-0.02}$	131(14)	0.281(8)
		3_1^-	700.2(3)	24.4(18)	0.08(10)		
3057.5(3)	2_5^+	0_1^+	n 3057.2(5)	8.16(66)	0	141(15)	0.267(8)
		2_1^+	2123.0(3)	39.1(21)	0.69(16)		
		0_2^+	n 1674.9(5)	3.71(47)	0		
		2_3^+	990.5(2)	100(27)	–		
		3_1^-	717.9(2)	31.5(19)	−0.03(7)		
3124.6(3)	$1_1^{(+)}$ n	0_1^+	3124.5(5)	31.4(18)	0	84(9)	0.377(5)
		2_1^+	n 2190.3(5)	27.3(17)	–		
		0_2^+	n 1741.6(3)	100.0(52)	0		
		2_3^+	1058.0(3)	49.3(27)	$-3.1^{+1.5}_{-5.9}$ −0.02(20)		

TABLE I. (*Continued*.)

E_x (keV)	J_i^π	J_f^π	E_γ (keV)	I_γ (%)	δ	τ (fs)	$F(\tau)$
3178.3(2)	4_4^+	2_1^+	2243.6(4)	25.8(15)	$0.06^{+0.10}_{-0.09}$	78(8)	0.404(8)
		4_2^+	779.9(2)	100.0(15)	−0.04(4)		
3191.0(3)	(4^-)	4_1^+	1695.5(3)	100.0	$-0.02^{+0.04}_{-0.03}$	221(26)	0.189(10)
3262.9(4)	2_6^+	0_1^+	3262.6(5)	29.3(17)	0	18(2)	0.751(5)
		2_1^+	2328.4(4)	100.0(17)	−0.06(3)		
3275.9(2)	3_2^+ n	2_1^+	2341.2(4)	27.1(16)	$4.4^{+0.8}_{-0.5}$	76(8)	0.409(8)
		2_2^+	n 1428.7(5)	4.2(5)	−		
		2_3^+	1209.4(2)	100.0(51)	−		
		4_2^+	877.5(2)	23.1(15)	>10		
					$0.08^{+0.04}_{-0.05}$		
3288.9(3)	(3^+)	2_1^+	2354.4(3)	100.0(54)	0.29(3)	251(28)	0.166(6)
		4_1^+	1793.4(3)	35.2(22)	0.22(5)		
		2_2^+	n 1441.6(5)	26.4(18)	0.24(5)		
		2_3^+	1222.2(4)	92.7(50)	$0.68^{+0.09}_{-0.07}$		
					2.31(35)		
		3_1^+	379.6(2)	77.9(44)	0.02(6)		
					1.5(2)		
3371.4(3)	$1_1^{(-)}$	0_1^+	3371.0(5)	42.8(27)	0	39(4)	0.578(8)
		2_1^+	2436.9(5)	43.1(26)	0.11(18)		
					$-5.2^{+2.5}_{-26.6}$		
		0_2^+	1988.6(3)	100.0(53)	0		
3407.8(3)	(2^-) n	2_1^+	2473.2(3)	73.2(40)	0.08(6)	428^{+57}_{-53}	0.106(7)
		3_1^-	1068.2(2)	100.0(40)	5.8(21)		
					$0.36^{+0.06}_{-0.05}$		
3452.1(3)	(2^+)	2_1^+	2517.6(4)	100.0(56)	2.0(12)	84(9)	0.386(9)
		4_1^+	1956.6(6)	35.9(27)	−		
		2_2^+	1604.9(3)	92.4(53)	$-1.5^{+0.5}_{-0.8}$		
		3	1112.5(8)	21.0(21)	−		
3463.2(5)	(4^+)	2_1^+	n 2528.7(5)	33.8(23)	0.11(10)	198^{+30}_{-25}	0.206(15)
		4_1^+	n 1967.7(5)	100.0(23)	−		
3472.1(5)	1_2^+	0_1^+	3471.9(5)	100.0(54)	0	7.6(9)	0.884(6)
		2_1^+	2537.5(5)	39.2(23)	$-3.4^{+1.7}_{-28}$		
					0.0(3)		
		0_2^+	2089.6(5)	17.9(14)	0		
3500.1(3)	2^+	0_1^+	3499.8(5)	100.0(54)	0	76(7)	0.411(8)
		2_1^+	n 2565.6(5)	15.8(13)	$-0.62^{+0.16}_{-0.27}$		
					$-6.5^{+3.4}_{-57}$		
		2_2^+	1652.8(3)	55.6(31)	$3.3^{+0.6}_{-0.4}$		
					$-0.11^{+0.03}_{-0.05}$		
		2_3^+	1433.6(4)	19.3(14)	−		
		3_1^-	n 1160.5(5)	22.4(18)	−0.04(15)		
n 3609.3(5)	(0^+) n	2_1^+	n 2674.8(5)	100.0(39)	−	218^{+38}_{-33}	0.191(21)
		2_2^+	n 1762.3(5)	29.3(39)	−		
3628.4(4)	(2,3)	2_1^+	2693.9(4)	100.0	−	37(4)	0.592(12)
3638.1(5)	1_2^-	0_1^+	3638.0(5)	100.0(16)	0	12.1(16)	0.828(11)
		0_2^+	2255.4(3)	14.1(16)	0		
3640.3(4)	(2^+)	2_1^+	2705.8(4)	100.0(26)	3.5(4)	184(21)	0.218(10)
					$-0.12^{+0.03}_{-0.04}$		

TABLE I. (*Continued.*)

E_x (keV)	J_i^π	J_f^π	E_γ (keV)	I_γ (%)	δ	τ (fs)	$F(\tau)$
		3_1^-	1300.8(8)	6.7(26)	–		
3649.2(4)	(3^+) n	2_1^+	2714.7(5)	73.2(51)	$-0.73^{+0.12}_{-0.18}$	81(10)	0.391(15)
		4_1^+	2153.7(5)	100.0(68)	$-3.90^{+0.65}_{-0.93}$		
					$-0.12(4)$		
		2_2^+	n 1801.8(5)	26.2(35)	$-3.8^{+0.9}_{-1.4}$		
					$-0.08(8)$		
		4_2^+	n 1250.8(3)	49.6(48)	$12.0^{+52}_{-5.7}$		
					$0.22^{+0.07}_{-0.08}$		
n 3675.8(4)	(5^+) n	4_1^+	n 2180.3(4)	100.0	$3.6^{+0.6}_{-0.5}$	168^{+34}_{-29}	0.235(29)
3696.6(7)	$1_3^{(+)}$ n	0_1^+	n 3696.5(7)	100.0(73)	0	25(4)	0.693(15)
		2_1^+	n 2762.3(4)	98.5(73)	$1.3^{+2.8}_{-0.8}$		
3774.4(5)	$1, 2^{(+)}$ n	0_1^+	n 3774.6(8)	45.6(92)	0	25(7)	0.658(52)
		2_1^+	n 2839.9(5)	100(20)	–		
		2_2^+	n 1927.1(5)	34.9(70)	–		
		2_3^+	n 1708.1(5)	49.1(98)	–		
n 3804.6(5)	?	2_1^+	n 2870.1(5)	100.0	–	13^{+8}_{-7}	0.810(89)
3830.6(5)	$(1^-, 2^+)$	2_1^+	2895.1(10)	100(18)	–	–	–
		3_1^+	1491.0(5)	92(18)	–		

III. LEVEL DISCUSSION

Experimental information for all observed levels is provided in Table I; the data for some states are discussed in detail below. New excited states were identified at 3609.3, 3675.8, and 3804.6 keV. In addition, excited states at 3463.2 and 3774.4 keV were detected for the first time in γ-ray spectroscopy.

2_2^+ state at 1847.3 keV. The spin and parity of this state were previously known [19] and were confirmed from our data. The branching ratio of the $2_2^+ \rightarrow 0_1^+$ and $2_2^+ \rightarrow 2_1^+$ transitions is in rather good agreement with the data from Ref. [19]. A lifetime of $\tau(2_2^+) = 138(14)$ fs was determined from the DSAM measurement with $E_n = 2.2$ MeV, in agreement with [7], reducing the error by a factor of 2. We obtained possible $E2/M1$ mixing ratios for the $2_2^+ \rightarrow 2_1^+$ transition of $\delta = -0.04(2)$ and $\delta = 2.6(2)$. We accept the first value because of its agreement with the result of an analysis of the $\gamma\gamma$-angular correlation of the cascade $2_2^+ \rightarrow 2_1^+ \rightarrow 0_1^+$ observed in the electron capture decay of ^{92}Nb to ^{92}Zr, which gave a value of $\delta = -0.013^{+0.041}_{-0.024}$ [29] using the Krane-Steffen-Wheeler convention [30]. This result for the mixing ratio is also in agreement with a $\gamma\gamma$-angular correlation study from β decay by Bunker *et al.* [31].

2_3^+ state at 2066.6 keV. In addition to the known $2_3^+ \rightarrow 2_1^+$ and $2_3^+ \rightarrow 2_2^+$ transitions, the ground-state transition was observed. A weak decay branch to the 4_1^+ state given in [19] was not identified in our spectra. For the $E2/M1$ mixing ratio of the $2_3^+ \rightarrow 2_1^+$ transition, we determined values of

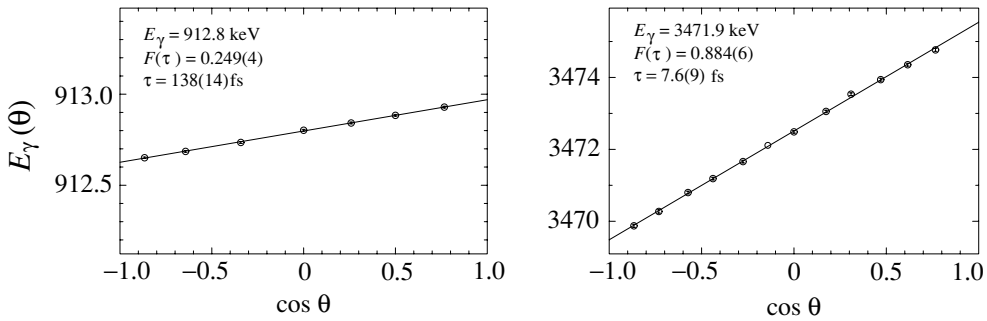

FIG. 3. Determination of lifetimes from Doppler shifts in the $(n,n'\gamma)$ angular distribution measurement. The diagram shows the Doppler shifts of the 912.8-keV $2_2^+ \rightarrow 2_1^+$ transition observed in the measurement with a neutron energy of $E_n = 2.2$ MeV and the ground-state decay of the 3472.1-keV state observed in the experiment with $E_n = 3.9$ MeV. Observed energies are shown as a function of the cosine of the γ-ray emission angle θ relative to the direction of the incident neutrons. The experimental value of the Doppler-shift attenuation factor $F(\tau)$ is determined from the slope of the best-fit line.

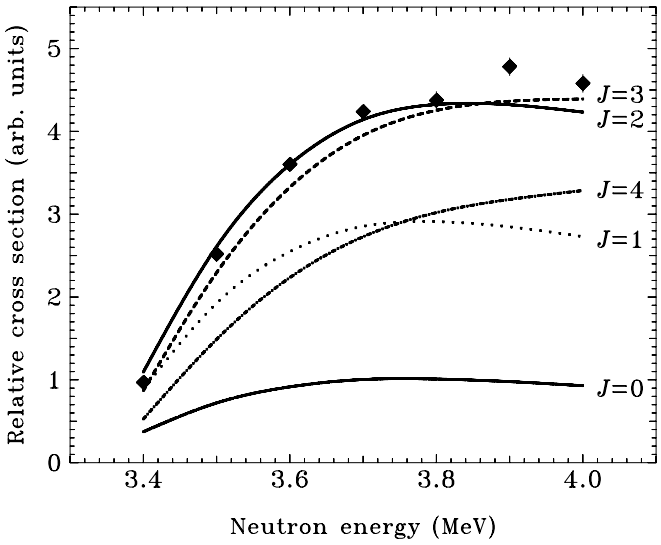

FIG. 4. Excitation function data for the 3262.9-keV level. The diagram displays a comparison of the experimental neutron scattering cross sections with the calculations from the code CINDY [24] for five different spin possibilities $J = 0-4$. A deviation of the data points for the two highest neutron beam energies from the calculated cross sections for $J = 2$, 3 possibly results from feeding of the 3262.9-keV level from an unobserved level at an excitation energy higher than 3.8 MeV.

$\delta = -3.2^{+0.5}_{-0.4}$ and $\delta = 0.85(7)$, which are consistent with the results of Glasgow *et al.* [21]. We accept the first mixing ratio, because it is in agreement with the value from an (n,γ) experiment of $\delta = -2.7^{+0.8}_{-1.5}$ [19]. Thus, the $2^+_3 \rightarrow 2^+_1$ transition has mainly $E2$ character.

4^+_2 state at 2398.4 keV. The spin and parity assignment from Ref. [19] was confirmed primarily as a result of the observation of a fast $E2$ transition to the 2^+_1 state. The $E2/M1$ mixing ratio of the $4^+_2 \rightarrow 4^+_1$ decay is $\delta = -0.11^{+0.03}_{-0.02}$; therefore, the transition has mainly $M1$ character. In Ref. [21], this mixing ratio was not measured unambiguously, but our result is close to one of the values, $\delta = 0.13(9)$, determined in that work. The different sign results from the different phase conventions used in this work and in Ref. [21].

2^+_4 state at 2819.6 keV. We were able to observe decay transitions to the 0^+_1, 2^+_1, and 2^+_2 states; however, an additional weak decay branch to the 0^+_2 state reported in Ref. [19] was not detected. A possible $2^+_4 \rightarrow 5^-_1$ decay, mentioned in [19] from an (n,γ) experiment, probably does not exist. This decay is reported to have about 12% of the intensity of the strong $2^+_4 \rightarrow 2^+_2$ decay [19], and it should have been observed in our measurements. $E2/M1$ mixing ratios of the $2^+_4 \rightarrow 2^+_1$ and $2^+_4 \rightarrow 2^+_2$ decays are ambiguous.

4^+_3 state at 2864.7 keV. The excitation energy of this state from our experiments is 1.3 keV higher than the energy given in Ref. [19]. Note that the energies of all the decay transitions observed here consistently result in the same level energy. In addition, the spin assignment of $J = 4$ is clear from the angular distribution data. The fast transition to the 2^+_1 state allows only positive parity. Besides the known decay transitions to the 2^+_1 and 4^+_1 states, a new $4^+_3 \rightarrow 4^+_2$ decay was observed. While the $4^+_3 \rightarrow 4^+_1$ transition has a mixing ratio of $\delta = -0.49(5)$, the $4^+_3 \rightarrow 4^+_2$ transition exhibits nearly pure $M1$ character.

0^+_3 state at 2904.0 keV. The known [19] decay transitions from this state to the 2^+_1 and the 2^+_3 states were observed, but the branching ratio of the $0^+_3 \rightarrow 2^+_1$ and $0^+_3 \rightarrow 2^+_3$ γ rays deviates by a factor of 2 from the data in Ref. [19]. We accept our value, because it was measured in the angular distribution experiment and independently checked with the excitation function data; therefore, we can exclude spectral interferences.

3^+_1 state at 2909.3 keV. A $2^+, 3^+$ state had been identified previously at 2909.46(8) keV [19]. The parity assignment arises from a ^{91}Zr$(d,p)^{92}$Zr experiment, in which an $l = 0$ transfer was determined for an excited state at 2911 keV [32]. As the ground state of ^{91}Zr is $J^\pi = 5/2^+$, this allows only $J^\pi = 2^+, 3^+$ for the state in ^{92}Zr. Since most energies in [32] were overestimated by about 2 keV, we identify the 2911-keV level with the state we observe at 2909.3 keV. From our measurements, we limit this state to have spin and parity $J^\pi = 3^+$. $J = 2$ can be excluded from the angular distribution of the transition to the 4^+_1 state. Similarly, $J = 4$ is not possible because of the angular distributions of the transitions to the 2^+_1 and 2^+_3 states. We confirm the positive parity assigned in [32] since the multipole mixing ratios of the decays to the 4^+_1 and 2^+_3 states are nonzero. Both these transitions are strong, thus $E3/M2$ mixed transitions can be excluded. We identify this state as the 3^+_1 state in ^{92}Zr. A decay transition to the 3^-_1 state, observed only in an (n,γ) experiment [19], was not detected.

$J = 3$ state at 3039.8 keV. This level was assigned previously as a $J = (2, 3)$ state [19]. From the angular distribution data of the γ ray to the 3^-_1 state, we obtain the spin assignment $J = 3$. $J = 4$ can be excluded from the angular distribution of the transition to the 2^+_1 state. Negative parity is preferred due to the small multipole mixing ratios of both decays, allowing them to be pure $E1$ transitions; thus, this state represents a candidate for the 3^-_2 state.

2^+_5 state at 3057.5 keV. Besides the known decay transitions [19], decays to the ground state and to the 0^+_2 state were established for the first time. The $2^+_5 \rightarrow 2^+_3$ transition forms a doublet with the $5^-_1 \rightarrow 4^+_1$ γ ray; therefore, the branching ratio given in Table I was taken from [19].

$1^{(+)}_1$ state at 3124.6 keV. New decays to the 2^+_1 and 0^+_2 states were observed in addition to the known decay branches from Ref. [19]. This state is indicated with $J^\pi = (1^+, 2^+)$ in Ref. [19]. The angular distributions of the γ ray to the 0^+_2 state and of the ground-state decay give clear evidence for $J = 1$. Positive parity was tentatively assigned to a level at 3126 keV from a ^{91}Zr$(d,p)^{92}$Zr experiment [32], and $l = 2$ transfer to this state was assigned. The angular distribution analysis of the emitted protons with the distorted-wave Born approximation in [32] lead to the tentative spin and parity assignment $J^\pi = (1^+ - 4^+)$, where the data were corrected for a contamination resulting from the ^{94}Zr$(d,p)^{95}$Zr reaction. Since we observed no other level at this energy, we identify the 3126-keV level from Ref. [32] with the $J = 1$ state at 3124.6 keV from our measurement and, therefore, assign $J^\pi = 1^{(+)}$.

4^+_4 state at 3178.3 keV. $J^\pi = 4^+$ from Ref. [19] was confirmed by the angular distribution data. The strongest decay to the 4^+_2 state represents a nearly pure $M1$ transition.

(4^-) state at 3191.0 keV. The angular distribution data of the lone decay transition to the 4_1^+ state yielded $J = 3, 4, 5$. For $J = 3$ or 5, positive parity is required because for both those hypotheses the multipole mixing ratio of the decay to the 4_1^+ state would be nonzero, and the fast decay to the 4_1^+ state prohibits a strong $M2$ admixture. For the spin hypothesis $J = 4$, our data yielded a multipole mixing ratio of $\delta = -0.02^{+0.04}_{-0.03}$, which is consistent with the data from the earlier $(n,n'\gamma)$ experiment [21] and allows negative parity. From the $l = 3 + 5$ transfer in a ^{91}Zr$(d,p)^{92}$Zr experiment, spin and parity $J^\pi = (1^- - 4^-)$ were assigned [32]. Thus, $J = 3$ and 5 can probably be excluded, and we confirm the tentative $J^\pi = (4^-)$ assignment from Ref. [19].

4^+ state at 3236.9 keV. This state has been observed in different measurements [19]. The sole decay γ ray to the 4_1^+ state, detected in these earlier experiments, is expected to be a doublet with the transition of the $J^\pi = 1^{(+)}$ state at 3124.6 keV to the 0_2^+ state. But our excitation function data clearly exclude an additional contribution to this decay; therefore, we cannot confirm the observation of this 4^+ state.

2_6^+ state at 3262.9 keV. Spin and parity $J^\pi = 2^+$ were assigned in a recent photon scattering experiment [7] and confirmed in this work. The $2_6^+ \rightarrow 2_1^+$ transition is a nearly pure $M1$ transition.

3_2^+ state at 3275.9 keV. This state was previously known as a state with $J^\pi = (2^+, 3)$ [19]. From our data, we assign spin and parity $J^\pi = 3^+$ from the angular distribution of the decay to the 2_1^+ state, and we interpret this state as the 3_2^+ state in ^{92}Zr. Parity information is provided by the decay transition to the 2_1^+ state, with a multipole mixing ratio of $\delta = 4.4^{+0.8}_{-0.5}$. This result excludes negative parity because the rather fast transition to the 2_1^+ state makes a $M2/E1$ mixed transition with a large $M2$ component very unlikely. No hint for a decay transition to the 3_1^+ state, as reported in an (n,γ) experiment [19], was observed. From the branching ratio of this decay [19], it should have been observable in our spectra; thus, a $3_2^+ \rightarrow 3_1^+$ transition as given in [19] is excluded.

$1_1^{(-)}$ state at 3371.4 keV. The spin was clearly assigned from the decay transitions to the 0_1^+ and 0_2^+ states and confirmed the recent photon scattering result [7]. The short lifetime of this state of $\tau = 39(4)$ fs determined in this experiment is consistent with that given in [7] if the newly observed transitions from the neutron scattering experiment are taken into account in these data. The multipole mixing ratio of the transition to the 2_1^+ state was not determined unambiguously. In a ^{91}Zr$(d,p)^{92}$Zr experiment, an $l = (3)$ transfer was measured for a level at 3374 keV, pointing to negative parity [32]. As mentioned above, the level energies in [32] are in most cases slightly overestimated. Thus, we identify this state with the state at 3371.4 keV from our measurements and assign $J^\pi = 1^{(-)}$.

(2^+) state at 3452.1 keV. This state was observed in previous experiments [19]. Our angular distribution data of the decays to the 2_1^+, 4_1^+, and 2_2^+ states allow the spin assigment $J = 2$, whereas the angular distribution of the decay to the 3_1^- state points slightly to $J = 3$, but in this case, low statistics prevent a clear spin assignment.

(4^+) state at 3463.2 keV. The γ rays from this state were observed in our experiments for the first time. From the angular distribution data, we make the tentative spin assignment $J = 3, 4$. The state can perhaps be identified with a (4^+) state at $\approx$3460 keV from Ref. [19]. The spin assignment comes from a ^{91}Zr$(d,p)^{92}$Zr experiment, where an $l = 2$ transfer was measured for an excited state at 3445 keV [33]. In addition, an $l = 4$ transfer was determined in the same work for an excited state at 3451 keV in the reaction ^{90}Zr$(t,p)^{92}$Zr, pointing to spin and parity 4^+. Since the energies in [33] are 5 to 10 keV low, we identify the state observed in our measurements with the state from [33] and tentatively assign $J^\pi = (4^+)$.

1_2^+ state at 3472.1 keV. The angular distribution data yield $J = 1$. This result is consistent with the data from a photon scattering experiment with unpolarized bremsstrahlung [7]. In a recently performed photon scattering experiment with the polarized photon beam from a free electron laser, positive parity was clearly assigned [20].

2^+ state at 3500.1 keV. The spin and parity, $J^\pi = 2^+$, from Ref. [19] were confirmed from the angular distribution data of the fast ground-state decay, giving $J = 2$ and prohibiting negative parity. Decay transitions to the 2_1^+ and 3_1^- states were observed for the first time. The branching ratio of the decay transitions to the 2_2^+ and 2_3^+ states from Ref. [19] was not confirmed by our work and should be revised, because a contamination of the corresponding γ-ray lines in our experiment is very unlikely. The rather weak decay transitions to the 2_4^+, 3_1^+, and 3_2^+ states from Ref. [19] were not observed in our experiments. $E2/M1$ mixing ratios of the decay transitions to the 2_1^+, 2_2^+, and 2_3^+ states are ambiguous. The lifetime of $\tau = 76(7)$ fs from this measurement is consistent with the value from Ref. [7], taking into account all decay branches from that level.

(0^+) state at 3609.3 keV. No spin or parity information was obtained from the angular distribution measurement. The excitation function data yield $J = (0)$, whereas we assume positive parity as a result of the rather strong decay transition to the 2_1^+ state.

1_2^- state at 3638.1 keV. This state was also identified from both its ground-state transition and its decays to the 2_1^+ and 0_2^+ states in a recent photon scattering experiment [7], which is in agreement with our data. Negative parity was assigned from the results of a recent experiment with a polarized photon beam [20].

(2^+) state at 3640.3 keV. The spin from Ref. [19] was confirmed from the angular distribution of the decay to the 2_1^+ state. The branching ratios of the decay transitions to the 2_1^+ and 3_1^- states from our measurement are in agreement with data from Ref. [19], but weaker decays [19] to the 2_4^+ state and a $J = 3$ state at 3039.8 keV (the placement in the level scheme in Ref. [19] is not clear) were not confirmed by our data.

(3^+) state at 3649.2 keV. $J = (3)$ was determined from the angular distribution data. From previous measurements, this level was known as a $(3, 4)^+$ state [19]. In a ^{91}Zr$(d,p)^{92}$Zr experiment, an excited state at 3655 keV was observed, for which $J^\pi = (1^+ - 4^+)$ was assigned due to an $l = 2$ transfer in the (d,p) reaction [32]. Since the energies in [32] were in general slightly overestimated and, except for the states around 3640 keV, no further states were observed in our measurements in this energy region, we identify the state from

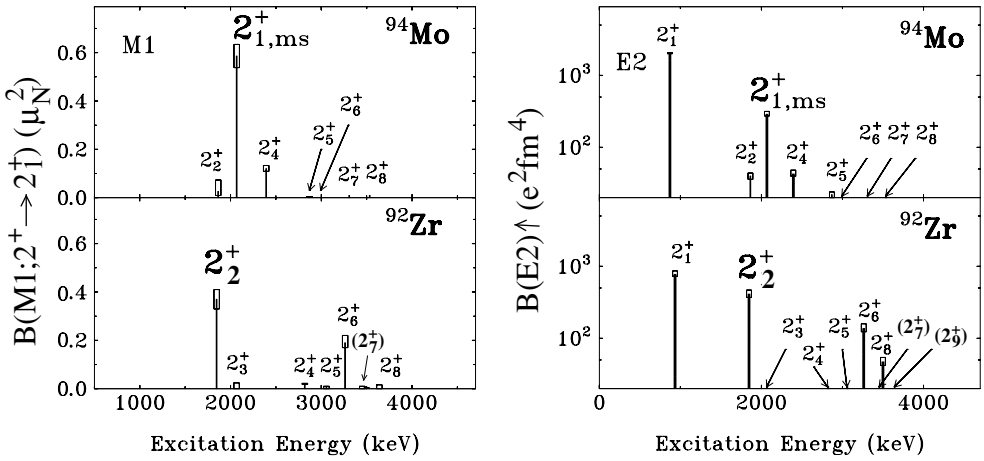

FIG. 5. Comparison of $M1$ transition strengths of all $2^+ \rightarrow 2^+_1$ transitions in ^{94}Mo (from [4]) and ^{92}Zr (left) and $E2$ ground-state transition strengths of all 2^+ states in the same nuclei (right) (data for ^{94}Mo from [4]). Both the 2^+_3 state in ^{94}Mo and the 2^+_2 state in ^{92}Zr decay with strong $M1$ transitions to the 2^+_1 state. The open boxes give the error bars.

[32] with the state at 3649.2 keV and assign possible positive parity.

$1^{(+)}$ state at 3696.6 keV. In agreement with a recent photon scattering experiment [7], we observed a $J = 1$ state at this energy. The branching ratio of the observed decay transitions to the ground state and the 2^+_1 state is in agreement with the photon scattering data [7]. An indication of positive parity is provided by the multipole mixing ratio of the fast decay to the 2^+_1 state of $\delta = 1.3^{+2.8}_{-0.8}$. Negative parity is prohibited because, if this were the case, the decay would have a mainly $M2$ character, which can be excluded. Additional evidence of positive parity arises from a ^{91}Zr$(d,p)^{92}$Zr experiment [32].

$1, 2^{(+)}$ state at 3774.4 keV. We tentatively assign $J = 1, 2$ to this state because of the fast ground-state transition. It was observed here for the first time in a γ-ray measurement. Due to low statistics, the angular distribution data do not allow the determination of multipole mixing ratios. $J^\pi = (1^+ - 4^+)$ was assigned to a state at 3781 keV in a ^{91}Zr$(d,p)^{92}$Zr experiment because of the measured $l = 2$ transfer [32]. Since we detected no further low-spin states in this energy range, we identify the state at 3774.4 keV with the state from [32]. Therefore, we prefer positive parity.

Excited state at 3804.6 keV. This state, newly observed in this work, was identified from its lone decay transition to the 2^+_1 state. Low statistics prevent a determination of the spin and multipole mixing ratio. This state may be the one observed at 3814 keV in the (d,p) experiment [32], for which the tentative spin assignment $J^\pi = (1^+ - 4^+)$ was made.

IV. DISCUSSION

A. Comparison to ^{94}Mo

Investigating the evolution of MS structures along the $N = 52$ isotonic chain represents the main motivation for our studies. The structure of the nucleus ^{92}Zr is particularly interesting because it lies at the proton subshell closure $Z = 40$, and strong shell effects must be expected to show up even in the properties of typically collective states, such as the 2^+_1 state, not to mention nonyrast structures such as MS states. Indeed, the $E2$ ground-state transition strength of the 2^+_1 state is strongly reduced at $Z = 40$ for $N = 52$ isotones. In ^{94}Mo, this transition exhibits a $B(E2; 2^+_1 \rightarrow 0^+_1)$ of 16.0(2) W.u., while it amounts to only $6.4^{+0.6}_{-0.5}$ W.u. in ^{92}Zr. In addition, the measured negative g factor of the 2^+_1 state [9] hints at an enhanced neutron contribution to this state and contradicts the interpretation as a fully pn symmetric collective state, for which one would expect a positive g factor of about Z/A. The amount of pn symmetry-breaking in the 2^+_1 and other low-spin states of ^{92}Zr has been debated in the literature [7,9,34]. It represents an important key to answering the question of whether or not excited structures of ^{92}Zr could be understood in a collective framework, such as the interacting boson model, or even in a simple phonon coupling scheme as was possible for the heavier $N = 52$ isotones. Indeed, it has been shown for ^{94}Mo that microscopic phenomenological models like the shell model [8] or the quasiparticle phonon model (QPM) [35] are able to reproduce the collective, pn symmetric or MS character of low-spin states. Competition between collective and single-particle structures is very pronounced in ^{92}Zr, and the structure of this nucleus sheds light on the evolution of collectivity in this mass region.

Assuming naively a sequential filling of spherical shell model orbitals, the proton $2p_{1/2}$ orbital is filled in the Zr isotopes, preventing $J_p = 2$ proton configurations at low energy. This should result in a dominance of neutron configurations in low-energy states, which has indeed been verified experimentally from g-factor measurements [9]. The structure of low-lying excited states in ^{92}Zr can be reproduced successfully within the shell model with a comparatively small proton configuration space [7,36].

On the other hand, collective structures with pronounced multiphonon character exist in neighboring nuclei with $Z > 40$, such as ^{94}Mo. It is, thus, interesting to compare the data for ^{94}Mo and ^{92}Zr. Figure 5 displays a comparison of the $M1$ and $E2$ strengths in ^{94}Mo and ^{92}Zr relevant for the identification of the dominant fragments of the one-quadrupole phonon $2^+_{1,\mathrm{ms}}$ state. Both data sets correspond to comparably

comprehensive spectroscopic information up to about 4 MeV. The $2^+ \rightarrow 2_1^+$ $M1$ and the $E2$ excitation strength distributions in ^{94}Mo and ^{92}Zr are surprisingly similar. The distribution of $B(E2; 0_1^+ \rightarrow 2^+)$ values is dominated in both nuclei by the 2_1^+ state, while one low-lying 2^+ state (the 2_3^+ state of ^{94}Mo and the 2_2^+ state of ^{92}Zr) carries the dominant part of the remaining strength. In both nuclei, it is just this nonyrast 2^+ state that completely dominates the $2^+ \rightarrow 2_1^+$ $M1$ strength distribution. In ^{92}Zr some fraction, both of the $E2$ as well as of this $M1$ distribution, is also carried by the 2_6^+ state. In ^{94}Mo, the 2_3^+ state was identified as the $2_{1,\mathrm{ms}}^+$ state [1,4] due to the strong $2_3^+ \rightarrow 2_1^+$ $M1$ decay with a transition strength of $B(M1; 2_3^+ \rightarrow 2_1^+) = 0.56(5)\,\mu_N^2$ corresponding to a transition matrix element of $\langle 2_1^+ \| M1 \| 2_{1,\mathrm{ms}}^+ \rangle = 1.67(5)\mu_N$ and due to a weakly collective $E2$ decay to the ground state as predicted in the IBM–2 [13]. The 2_2^+ state of ^{92}Zr has similar characteristics as shown in Fig. 5. A strong $M1$ decay with $B(M1; 2_2^+ \rightarrow 2_1^+) = 0.37(4)\,\mu_N^2$, which corresponds to an $M1$ transition matrix element of $\langle 2_1^+ \| M1 \| 2_{1,\mathrm{ms}}^+ \rangle = 1.36(7)\,\mu_N$, and a $2_2^+ \rightarrow 0_1^+$ $E2$ decay with a transition strength of $B(E2; 2_2^+ \rightarrow 0_1^+) = 3.4(4)$ W.u. were detected. The surprisingly small impact of the difference in proton number ($Z = 40$ for ^{92}Zr versus $Z = 42$ for ^{94}Mo) on these strength distributions indicates a rather robust structure of this 2^+ state that dominates the $M1$ strength distribution. This is interesting because a smooth dependence on nucleon number is one signature for collective structures and, hence, a collective interpretation of that state even in ^{92}Zr might be likely. Note that this state which dominates the $2^+ \rightarrow 2_1^+$ $M1$ strength distribution is the 2_2^+ state of ^{92}Zr, whereas it is the 2_3^+ state of ^{94}Mo. The energies of the state having this structure and of that with a predominantly two-phonon character invert when going from ^{94}Mo to ^{92}Zr. Mixing between these two structures is surprisingly small, as is evident from the small values for the $B(E2; 2_3^+ \rightarrow 0_1^+)$ and $B(M1; 2_3^+ \rightarrow 2_1^+)$ values in ^{92}Zr in comparison to those for the nearby 2_2^+ state. The interpretation of the 2_3^+ state of ^{92}Zr as having a predominantly two-phonon character is supported by the large $E2$ admixture in the transition to the 2_1^+ state.

In order to attempt an interpretation of the 2_2^+ state of ^{92}Zr, we note that it exhibits very similar properties, even quantitatively, to those of the 2_3^+ state of the isotone ^{94}Mo, which has been identified as the $2_{1,\mathrm{ms}}^+$ state of that nuclide from detailed comparison to the predictions of the IBM–2. The corresponding assignment of the 2_2^+ state of ^{92}Zr as the $2_{1,\mathrm{ms}}^+$ state would be hampered by the fact that a description of ^{92}Zr in the F-spin limit of the IBM–2 would be far too simplistic, and the microscopic structure of the wave functions are disputed in the recent literature. Based on our observations, it seems safe to consider the 2_2^+ state of ^{92}Zr as that structure which evolves into the $2_{1,\mathrm{ms}}^+$ state of ^{94}Mo when two more protons are added to the valence shell.

States with clear signatures of two-phonon MS states resulting from a coupling of the one-phonon pn symmetric 2_1^+ and the MS $2_{1,\mathrm{ms}}^+$ states were identified in ^{94}Mo from their strong $M1$ transitions to the pn symmetric two-phonon states, their collective $E2$ transitions to the $2_{1,\mathrm{ms}}^+$ state, and their weakly collective $E2$ transitions to the 2_1^+ state.

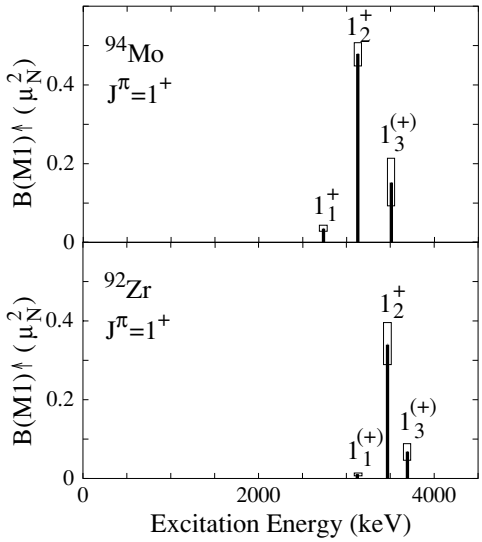

FIG. 6. $M1$ excitation strength distributions in ^{94}Mo and ^{92}Zr versus excitation energy below 4 MeV. The 1_2^+ state exhibits the strongest $M1$ excitation strength observed in both nuclei. The error bars are displayed as boxes.

Figure 6 shows the $M1$ excitation strength distributions in ^{92}Zr and ^{94}Mo [1,4]. Parities of strong dipole excitations in ^{92}Zr have recently been assigned unambiguously, as discussed above. These $M1$ excitation strength distributions are very similar. In ^{92}Zr, the total $M1$ excitation strength below 4 MeV amounts to $0.42^{+0.05}_{-0.04}\mu_N^2$ compared to $0.67(7)\ \mu_N^2$ in ^{94}Mo; however, the center of gravity of the $M1$ distribution shifts from 3.2 MeV in ^{94}Mo to about 3.5 MeV in ^{92}Zr. The 1_2^+ state at 3472.1 keV exhibits the strongest $M1$ excitation strength from the ground state of all 1^+ states observed in our experiment on ^{92}Zr, with an excitation strength of $B(M1; 0_1^+ \rightarrow 1_2^+) = 0.34(5)\,\mu_N^2$. Its decay scheme is shown in Fig. 7 in more detail. Besides the ground-state decay, an $M1$ decay to the 0_2^+ state with a transition matrix element of $|\langle 0_2^+ \| M1 \| 1_2^+ \rangle| = 0.53(8)\,\mu_N$ was observed. This 1_2^+ state also decays to the 2_1^+ state. Under the assumption of pure $E2$ radiation for the $1_2^+ \rightarrow 2_1^+$ decay, the transition strength is $B(E2; 1_2^+ \rightarrow$

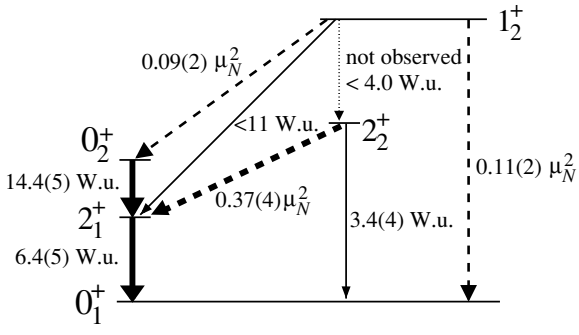

FIG. 7. Decay transitions of the 1_2^+ state at 3472 keV. $M1$ transition strengths (dashed lines) are given in μ_N^2; $E2$ transition strengths (solid lines) are in Weisskopf units. A $1_2^+ \rightarrow 2_2^+$ decay transition was not observed; therefore, the upper limit for the $E2$ transition strength is given.

TABLE II. Parameters of the SDI Hamiltonian for ^{92}Zr. The ϵ_x^ρ values are the single-particle energies for protons or neutrons in orbital x, and the $A^T_{\rho\rho'}$ values are the interaction parameters. The e_ρ values are the effective $E2$ charges, and the orbital and spin g factors are given by g_ρ^σ.

$\epsilon^p_{g_{9/2}}$	$\epsilon^p_{p_{1/2}}$	$\epsilon^n_{d_{5/2}}$	$\epsilon^n_{s_{1/2}}$	$\epsilon^n_{g_{7/2}}$	$\epsilon^n_{d_{3/2}}$	$\epsilon^n_{h_{11/2}}$	$A^{T=1}_{pp}$	$A^{T=1}_{nn}$	$A^{T=1}_{pn}$	$A^{T=0}_{pn}$
[MeV]										
0.0	−0.7	0.0	1.5	1.9	2.0	3.5	0.31	0.24	0.27	0.20
e_p		e_n		g^l_p		g^l_n		g^s_p		g^s_n
2.1		1.1		1		0		3.7983		−2.6019

$2^+_1) = 9.5^{+2.0}_{-2.6}$ W.u. A decay transition to the 2^+_2 state has not been observed. Such a transition is expected (as a collective $E2$ transition with a strength comparable to that of the $2^+_1 \to 0^+_1$ decay) if the 2^+_2 and the 1^+_2 states are interpreted as one-phonon and two-phonon states with an MS character. The $1^+_2 \to 2^+_2$ transition is suppressed with respect to the other decays because of the comparatively low transition energy. From the sensitivity limit of our measurements, we can infer an upper limit for the corresponding $E2$ decay strength of $B(E2; 1^+_2 \to 2^+_2) < 4$ W.u., which is smaller than the $B(E2; 2^+_1 \to 0^+_1)$ value but still not in severe disagreement with a multiphonon picture.

Also, a rather strong transition was observed from the 3^+_2 state to the 2^+_3 state with a predominantly two-phonon character. A dominant $E2$ character is very unlikely because of an unreasonably large $E2$ strength in that case. Under the assumption of pure $M1$ radiation, a transition strength of $B(M1; 3^+_2 \to 2^+_3) = 0.27(4)\,\mu_N^2$ was determined [i.e., the upper limit of the $M1$ transition strength amounts to $B(M1; 3^+_2 \to 2^+_3) < 0.31\,\mu_N^2$]. Thus, the data yield an $M1$ transition matrix element of $\langle 2^+_3 \| M1 \| 3^+_2 \rangle = 1.37(10)\,\mu_N$, in the case of a pure $M1$ transition. None of the other observed 3^+ states has a comparably strong transition to the 2^+_3 state or to the 4^+_1 state.

In addition, the $3^+_2 \to 2^+_1$ decay represents a weakly collective $E2$ transition with $B(E2; 3^+_2 \to 2^+_1) = 1.03^{+0.15}_{-0.13}$ W.u. Both transitions are expected with the observed strength for a two-phonon MS interpretation of the 3^+_2 state [34]. For a two-phonon MS state, a collective $E2$ transition to the $2^+_{1,\mathrm{ms}}$ state is also expected, but that decay was not observed if we accept the 2^+_2 state as the dominant fragment of the $2^+_{1,\mathrm{ms}}$ state. Our data yield a weak $3^+_2 \to 2^+_2$ transition, with an $E2$ strength of $B(E2; 3^+_2 \to 2^+_2) = 2.0(3)$ W.u., even assuming pure $E2$ radiation. Moreover, the 3^+_2 state decays rather strongly to the 4^+_2 state. This transition could be understood in the phonon picture (as a MS two-phonon to symmetric two-phonon transition) if the 4^+_2 state indeed shares a considerable portion of the symmetric two-phonon configuration. Indeed, the $E2$ decay of the 4^+_2 state to the 2^+_1 state has a strength of 6.1(8) W.u. and is even stronger than the $4^+_1 \to 2^+_1$ transition with a strength of $B(E2; 4^+_1 \to 2^+_1) = 4.05(11)$ W.u. Considerable fragmentation of the symmetric 4^+ two-phonon strength is expected for ^{92}Zr from a recent QPM calculation [34]. From our observations, we conclude that the wave functions of the 3^+_2 and 1^+_2 states probably contain considerable components of MS two-phonon states. However, quantitative deviations from the simple phonon coupling scheme indicate the presence of important configurations in the wave functions that are beyond a simple collective multiphonon picture.

B. Shell model results

We have attempted to describe these observations in terms of the shell model using ^{88}Sr as the inert core. This choice results in the configurational space spanned by two protons and two neutrons freely occupying the orbitals $\pi(2p_{1/2})$, $\pi(1g_{9/2})$, $\nu(2d_{3/2})$, $\nu(3s_{1/2})$, $\nu(1g_{7/2})$, $\nu(2d_{3/2})$, and $\nu(1h_{11/2})$. The surface delta interaction (SDI) was used as the residual interaction. Parameters for ^{92}Zr have been derived in [7]. These parameters have been optimized [37] for the presently available data, enhancing especially the description of g factors and transition strengths. The single-particle energies, interaction parameters, and effective charges which were input for the code RITSSCHIL [38] are given in Table II.

Figure 8 shows calculated versus experimental level energies for positive parity low-spin states up to 3.5 MeV. The overall level pattern is well reproduced. Experimental transition rates of some levels are given in Table III and compared to the model predictions. Those levels are discussed below.

1. $J^\pi = 0^+$ states

The results from the new calculation for the ground state and the first excited 0^+ state are similar to the findings given in Ref. [7], i.e., both states are strongly mixed with respect to the contributions from the $\pi(p_{1/2})$ and $\pi(g_{9/2})$ orbitals. From the qualitative agreement between the decay behaviors of the shell model $0^+_{4,\mathrm{SM}}$ state and the experimental $0^+_{3,\mathrm{exp}}$ state (much stronger $E2$ decay to the $2^+_{3,\mathrm{exp}}$ state than to the $2^+_{1,\mathrm{exp}}$ state; see Table III), one might conclude that these two levels are interchanged in the calculation.

2. $J^\pi = 1^+$ states

The first 1^+ state in the shell model calculation, the $1^+_{1,\mathrm{SM}}$ state, dominates the calculated $M1$ strength distribution with a ground-state transition strength of 0.13 μ_N^2, while the third $1^+_{3,\mathrm{SM}}$ state also shows a considerable ground-state

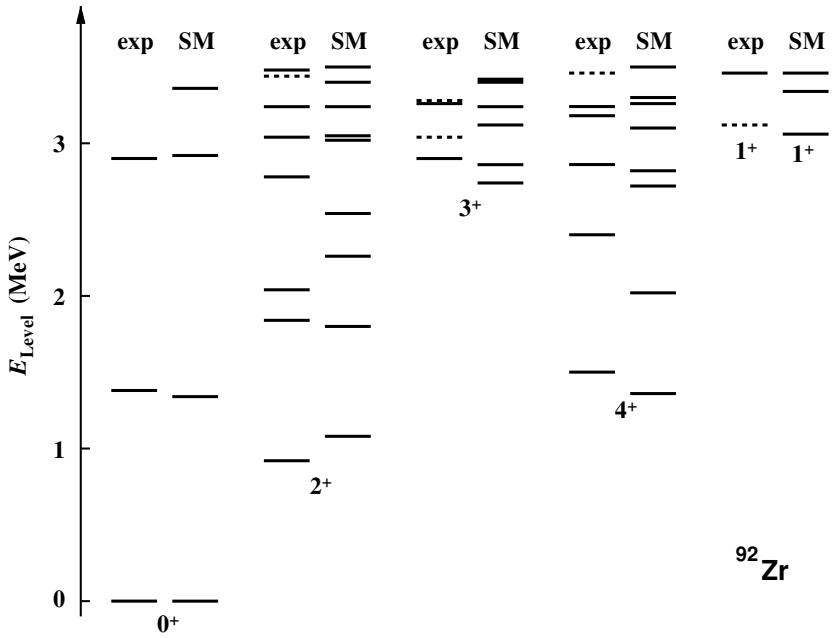

FIG. 8. Measured (exp) and calculated (SM) excitation energies of positive parity states with spin $J = 0, \ldots, 4$. Dashed lines indicate states with unassigned parity.

transition strength of 0.08 μ_N^2, being roughly 300 keV higher in energy. While the calculated energy of the $1^+_{1,\text{SM}}$ state is close to the excitation energy of the $1^{(+)}_{1,\text{exp}}$ state, its decay pattern better matches the one observed for the $1^+_{2,\text{exp}}$ state at 3472.1 keV, including the comparatively strong decay to the $0^+_{2,\text{exp}}$ state (see Table III). The dominant components of the $1^+_{1,\text{SM}}$ wave function are 54.8% $\pi(g^2_{9/2})_2\nu(d^2_{5/2})_2$, 23.7% $\pi(g^2_{9/2})_4\nu(d^2_{5/2})_4$, and 9.6% $\pi(g^2_{9/2})_0\nu(d^1_{5/2}d^1_{3/2})_1$. We see that $j = 4$ contributions to the $1^+_{1,\text{SM}}$ state are large. This may be responsible for some deviations from the behavior expected for a mixed-symmetric two-phonon state. In fact, $j = 4$ couplings of valence nucleons seem to play an important role at low energies for ^{92}Zr, as is also seen in the lowest-lying 4^+ states with the large $M1$ strength between both. Both orbital and spin parts of the $M1$ transition operator contribute appreciably to the $M1$ matrix element for the ground-state decay of the 1^+ state. The pure spin $B(M1)\downarrow_\sigma$ value (using vanishing orbital g factors $g^l_p = g^l_n = 0$) would amount to 0.066 μ_N^2. The pure orbital $B(M1)\downarrow_l$ value (using vanishing spin g factors $g^s_p = g^s_n = 0$) would amount to 0.012 μ_N^2.

3. $J^\pi = 2^+$ states

The 2^+_1 state of a heavy even-even nucleus is typically a pn symmetric state. This is not the case for ^{92}Zr, according to the shell model calculation in this configurational space [7]. Since a $J_p = 2$ coupling is impossible for the valence protons occupying the $\pi(2p_{1/2})$ orbital, the proton contribution to the 2^+_1 state is suppressed in the shell model in agreement with the negative g factor of $g(2^+_1) = -0.18(1)$ [9]. This value can be reproduced by a reduction of the pn interaction in the SDI with respect to the value found for ^{94}Mo [8]. This weaker pn interaction results in a *partial* decoupling of proton and neutron excitations. The strong $M1$ matrix element connecting the two lowest 2^+ states indicates, however, that both proton configurations and neutron configurations are still important parts of their wave functions. These states represent the building blocks of what are the one-phonon symmetric and MS one-phonon states in the heavier $N = 52$ isotones. Here, they do not form fully symmetric and MS states, nor can they be identified with pure neutron and pure proton configurations, because in the latter case an $M1$ transition between the two states would not occur. There are proton contributions to the wave function of the 2^+_1 state, and even larger neutron contributions to the wave function of the 2^+_2 state, for which the calculations otherwise show a dominant proton character. Hence, the g factor of the 2^+_2 state is predicted to be positive and very large, $g(2^+_{2,\text{SM}}) = 1.07$, from the present calculation.

Both orbital and spin parts of the $M1$ transition operator contribute considerably to the $M1$ matrix element for the $2^+_2 \to 2^+_1$ transition. The pure spin $B(M1)\downarrow_\sigma$ value (using vanishing orbital g factors $g^l_p = g^l_n = 0$) would amount to 0.07 μ_N^2. The pure orbital $B(M1)\downarrow_l$ value (using vanishing spin g factors $g^s_p = g^s_n = 0$) would also amount to 0.07 μ_N^2. In contrast, the $2^+_{6,\text{exp}}$ state at 3263 keV, which has been identified above as the second strongest state of the $2^+ \to 2^+_1$ $M1$ distribution, possesses, according to the shell model, an appreciable $M1$ matrix element to the 2^+_1 state due to a $\nu(d_{3/2}) \to \nu(d_{5/2})$ spin-flip between the neutron d orbitals. This analysis is at variance with the recently suggested interpretation of this state as the first example of a **three-phonon** MS state from the results of a QPM calculation [34].

4. $J^\pi = 3^+$ states

The $3^+_{1,\text{exp}}$ state at 2909 keV is the most promising candidate for a state with a partial three-quadrupole phonon character. It decays through comparatively strong $E2$ transitions to the

TABLE III. Comparison of experimentally determined transition strengths and results from calculations in the spherical shell model with a surface delta interaction with the ^{88}Sr core for some low-lying excited states in ^{92}Zr.[a]

J_i^π	J_f^π	Experiment		Shell model [34]	
		$B(M1)$ (μ_N^2)	$B(E2)$ (W.u.)	$B(M1)$ (μ_N^2)	$B(E2)$ (W.u.)
2_1^+	0_1^+		$6.4^{+0.6}_{-0.5}$		6.2
0_2^+	2_1^+		14.4(5)		3.5
4_1^+	2_1^+		4.05(11)		4.2
2_2^+	0_1^+		3.4(4)		3.0
	2_1^+	0.37(4)	$0.4^{+0.5}_{-0.3}$	0.29	0.3
2_3^+	0_1^+		<0.005		0.2
	2_1^+	<0.024	<16	0.03	12.0
	2_2^+	<0.04	<430	0.18	0.9
4_2^+	2_1^+		6.1(8)		2.4
	4_1^+	0.26(3)	2.3(11)	0.47	0.1
0_3^+	2_1^+		0.28(12)		3.5
	2_3^+		47(19)		4.9
0_4^+	2_1^+				0.28
	2_3^+				9.3
3_1^+	2_1^+	<0.01	<1.8	0.01	0.02
	4_1^+	0.007(2) 0.018(3)	4.5(8) 1.3(4)	0	7.6
	2_2^+	–	–	0.002	0.2
	2_3^+	0.06(1)	$3.0^{+2.7}_{-1.6}$	0.09	3.6
3_2^+	2_1^+	0.0002(1)	$1.03^{+0.15}_{-0.13}$	0.01	2.7
	2_2^+	<0.008	<2.3	–	–
	2_3^+	<0.31	<124	0.29	2.7
	4_2^+	0.16(2)	$0.8^{+1.1}_{-0.7}$	0.07	2.2
		0	125^{+17}_{-15}		
1_2^+	0_1^+	0.11(2)		0.13	
	2_1^+	$0.01^{+0.02}_{-0.01}$ 0.11(2)	$9.5^{+2.0}_{-2.6}$	0.05	1.8
	0_2^+	0.09(2)		0.13	

[a]If no multipole mixing ratio for a γ-ray transition was determined experimentally, upper limits for the $M1$ and $E2$ transition strengths are given, which were calculated assuming pure dipole and quadrupole transitions, respectively. For the 2_3^+ state, the experimental data yielded only a lower limit for the lifetime, thus upper limits for the transition strengths are given, too. In some cases, the determination of the multipole mixing ratio was ambiguous, thus the transition strengths are quoted for both values (from Table I).

$4^+_{1,\mathrm{exp}}$ and $2^+_{3,\mathrm{exp}}$ states that themselves contain parts of the two-quadrupole phonon configurations. The $3^+_{3,\mathrm{SM}}$ state from the shell model reproduces the decay pattern of this level quantitatively.

The $3^+_{2,\mathrm{exp}}$ state at 3276 keV has been discussed above as a candidate for a fragment of the two-phonon MS 3^+_{ms} state. The shell model decribes the decays of this level quantitatively. The dominant components of the $3^+_{2,\mathrm{SM}}$ wave function are 46.9% $\pi(g^2_{9/2})_2\nu(d^2_{5/2})_2$, 10.0% $\pi(g^2_{9/2})_2\nu(d^1_{5/2}s^1_{1/2})_{(2,3)}$, and 8.5% $\pi(p^2_{1/2})_0\nu(d^1_{5/2}s^1_{1/2})_3$. Note the similarity of the dominant component with the one for the wave function of the $1^+_{1,SM}$ state. Both orbital and spin parts of the $M1$ transition operator contribute considerably to the $M1$ matrix element of the $3^+_{2,\mathrm{SM}}$ to 2^+_3 transition. The pure spin $B(M1)\downarrow_\sigma$ value is 0.10 μ_N^2. The pure orbital $B(M1)\downarrow_l$ value amounts to 0.05 μ_N^2.

5. $J^\pi = 4^+$ states

An exciting result of this work is finding a large $M1$ transition strength between the two lowest excited 4^+ states and comparably strong $E2$ transitions to the 2^+_1 state from both. The $M1$ decay was predicted in previous shell model calculations [7,8], while the current enhanced calculation addresses the data even better. The g factor of $g(4^+_{1,\mathrm{exp}}) = -0.5(1)$ [9] is well reproduced by the calculation, giving $g(4^+_{1,\mathrm{SM}}) = -0.38$, while for the 4^+_2 state a positive value of $g(4^+_{2,\mathrm{SM}}) = 1.15$ is predicted. The $M1$ strength between the two states is predicted to be 0.47 μ_N^2, close to the large experimental value of 0.26(3) μ_N^2 but still overpredicted by about a factor of 2.

The structures of the lowest 4^+ states show strong similarities to those of the two lowest 2^+ states. For the 2^+ states, strong $E2$ transitions to the 0^+_1 state and a large $M1$ transition between these states is observed; for the 4^+ states, strong $E2$ transitions to the 2^+_1 state and a large $M1$ transition between these states occur. In fact, their wave functions are also similar.

These wave functions should be examined in greater detail. For simplicity, we restrict ourselves to senority $\sigma = 2$ parts of the wave functions in which both protons or neutrons are in the same orbitals. For neutrons, we consider only the $d_{5/2}$ orbital, as other contributions are much smaller. For the protons, due to the large mixing between the $(p^2_{1/2})_0$ and $(g^2_{9/2})_0$ configurations, both were taken into account. For the $2^+_{1,\mathrm{SM}}$ state, we get a squared amplitude of the $[\pi(p^2_{1/2})_0\nu(d^2_{5/2})_2]_2$ and $[\pi(g^2_{9/2})_0\nu(d^2_{5/2})_2]_2$ configurations combined of 76%, and for the $2^+_{2,\mathrm{SM}}$ state the amplitude of the $[\pi(g^2_{9/2})_2\nu(d^2_{5/2})_0]_2$ configuration is 55%. These configurations are most similar to what are neutron and proton d bosons in the language of the IBM. The main components of the 4^+ wave functions are very similar, i.e., the portion of the $[\pi(p^2_{1/2})_0\ \nu(d^2_{5/2})_4]_4$ and $[\pi(g^2_{9/2})_0\nu(d^2_{5/2})_4]_4$ configurations in the $4^+_{1,\mathrm{SM}}$ state is 91%, and the portion of the $[\pi(g^2_{9/2})_4\nu(d^2_{5/2})_0]_4$ configuration in the $4^+_{2,\mathrm{SM}}$ state is 61%. Again, these correspond to what are usually taken as neutron or proton g-boson configurations, while only the main parts of the wave functions are given here. We note, however, that the $4^+_{4,\mathrm{exp}}$ state at 3178 keV shows an even larger $M1$ transition strength to the $4^+_{2,\mathrm{exp}}$ state with a value $B(M1; 4^+_4 \to 4^+_2) = 1.22^{+0.14}_{-0.12}\mu_N^2$.

Interestingly, an $M1$ transition was also observed in ^{94}Mo between the 4^+_2 and the 4^+_1 states with a remarkable strength of 1.2(2) μ_N^2 [4]. A new shell model calculation for ^{94}Mo based on the one presented here predicts an $M1$ strength of 1.3 μ_N^2 for the $4^+_{3,\mathrm{SM}} \to 4^+_{1,\mathrm{SM}}$ transition, and 0.1 μ_N^2 for the $4^+_{2,\mathrm{SM}} \to 4^+_{1,\mathrm{SM}}$ transition [37]. Thus, the $4^+_{2,3}$ states, which

are close in energy, are probably interchanged in the model calculation for ^{94}Mo.

The somewhat better description of transition strengths in ^{94}Mo may give a hint that in this case the quite strongly restricted shell model space chosen for the protons does not affect the description as much as it does in the case of ^{92}Zr, due to the different number of protons. Of course, the influence of lower-lying proton orbitals can only effectively be taken into account by tuning effective parameters in our shell model calculation. Nevertheless, the prediction of the most prominent features like strong $M1$ transitions between low-lying states (also for ^{92}Zr) shows that a major part of the structure is well reproduced in this restricted space.

A recent QPM calculation [34] for ^{92}Zr underpredicted the $B(E2; 4_1^+ \rightarrow 2_1^+)$ value by a factor of 4 and failed to reproduce the negative sign of the g factor of the 4_1^+ state. The authors argued [34] that instead the calculated 4_2^+ state should be associated with the observed 4_1^+ state, since the results for that QPM state—in particular, its negative g factor and the large $E2$ strength to the 2_1^+ state—better matched the observations for the 4_1^+ state. Our new data show, however, that actually the 4_2^+ state of ^{92}Zr has an even larger $E2$ transition strength to the 2_1^+ state. This observation is in contradiction with that reinterpretation of the lowest 4^+ QPM states. We hope that the new, comprehensive data, such as that presented here, might encourage the community to find an improved understanding of the formation of collective structures in this mass region.

V. SUMMARY

A detailed investigation of the low-spin level scheme of ^{92}Zr has been performed with the $(n,n'\gamma)$ reaction. Comprehensive data on level energies, spin and parity assignments, and electromagnetic decay properties were obtained. The complex data enable us to discuss structures that contain collective features such as one-phonon and two-phonon states with a predominantly pn symmetric or mixed-symmetric character, although the proton subshell closure at $Z = 40$ results in a much stronger perturbation of a simple collective phonon structure than in the heavier even-even isotone ^{94}Mo. Shell model calculations for ^{92}Zr using a ^{88}Sr core are in reasonable agreement with many of the observations and help identify the most important microscopic contributions to collective structures in this mass region.

ACKNOWLEDGMENTS

We acknowledge discussions with F. Iachello and U. Kneissl. We thank H. E. Baber for the smooth operation of the electrostatic accelerator of the University of Kentucky. This work was supported by the U. S. National Science Foundation under Grant Nos. PHY-0098813, PHY-0245018, and PHY-0354656 and by the Deutsche Forschungsgemeinschaft under Grants No. Pi 393/1-2 and Jo 391/3-1.

[1] N. Pietralla, C. Fransen, D. Belic, P. von Brentano, C. Friessner, U. Kneissl, A. Linnemann, A. Nord, H. H. Pitz, T. Otsuka, I. Schneider, V. Werner, and I. Wiedenhöver *et al.*, Phys. Rev. Lett. **83**, 1303 (1999).

[2] N. Pietralla, C. Fransen, P. von Brentano, A. Dewald, A. Fitzler, C. Friessner, and J. Gableske, Phys. Rev. Lett. **84**, 3775 (2000).

[3] C. Fransen, N. Pietralla, P. von Brentano, A. Dewald, J. Gableske, A. Gade, A. F. Lisetskiy, and V. Werner, Phys. Lett. **B508**, 219 (2001).

[4] C. Fransen, N. Pietralla, Z. Ammar, D. Bandyopadhyay, N. Boukharouba, P. von Brentano, A. Dewald, J. Gableske, A. Gade, J. Jolie, U. Kneissl, S. R. Lesher, A. F. Lisetskiy, M. T. McEllistrem, M. Merrick, H. H. Pitz, N. Warr, V. Werner, and S. W. Yates *et al.*, Phys. Rev. C **67**, 024307 (2003).

[5] N. Pietralla, C. J. Barton III, R. Krücken, C. W. Beausang, M. A. Caprio, R. F. Casten, J. R. Cooper, A. A. Hecht, H. Newman, J. R. Novak, and N. V. Zamfir *et al.*, Phys. Rev. C **64**, 031301(R) (2001).

[6] H. Klein, A. F. Lisetskiy, N. Pietralla, C. Fransen, A. Gade, and P. von Brentano, Phys. Rev. C **65**, 044315 (2002).

[7] V. Werner, D. Belic, P. von Brentano, C. Fransen, A. Gade, H. von Garrel, J. Jolie, U. Kneissl, C. Kohstall, A. Linnemann, A. F. Lisetskiy, N. Pietralla, H. H. Pitz, M. Scheck, K.-H. Speidel, F. Stedile, and S. W. Yates *et al.*, Phys. Lett. **B550**, 140 (2002).

[8] A. F. Lisetskiy, N. Pietralla, C. Fransen, R. V. Jolos, and P. von Brentano, Nucl. Phys. **A677**, 100 (2000).

[9] G. Jakob, N. Benczer-Koller, J. Holden, G. Kumbartzki, T. J. Mertzimekis, K.-H. Speidel, C. W. Beausang, and R. Krücken, Phys. Lett. **B468**, 13 (1999).

[10] A. Arima, T. Otsuka, F. Iachello, and I. Talmi, Phys. Lett. **B66**, 205 (1977).

[11] T. Otsuka, Ph.D. thesis, University of Tokyo, 1978; F. Iachello, lecture notes on theoretical physics, Groningen, 1976.

[12] T. Otsuka, A. Arima, and F. Iachello, Nucl. Phys. **A309**, 1 (1978).

[13] F. Iachello, Phys. Rev. Lett. **53**, 1427 (1984).

[14] G. Siems, U. Neuneyer, I. Wiedenhöver, S. Albers, M. Eschenauer, R. Wirowski, A. Gelberg, P. von Brentano, and T. Otsuka, Phys. Lett. **B320**, 1 (1994).

[15] T. Otsuka and K. H. Kim, Phys. Rev. C **50**, 1768(R) (1994).

[16] N. Pietralla, T. Mizusaki, P. von Brentano, R. V. Jolos, T. Otsuka, and V. Werner, Phys. Rev. C **57**, 150 (1998).

[17] N. Pietralla, P. von Brentano, R.-D. Herzberg, U. Kneissl, N. Lo Iudice, H. Maser, H. H. Pitz, and A. Zilges, Phys. Rev. C **58**, 184 (1998).

[18] P. van Isacker, K. Heyde, J. Jolie, and A. Sevrin, Ann. Phys. (NY) **171**, 253 (1986).

[19] C. M. Baglin, Nucl. Data Sheets **91**, 423 (2000).

[20] C. Fransen, N. Pietralla, A. P. Tonchev, M. W. Ahmed, J. Chen, G. Feldman, U. Kneissl, J. Li, V. Litvinenko, B. Perdue, I. V. Pinayev, H. H. Pitz, R. Prior, K. Sabourov, M. Spraker, W. Tornow, H. R. Weller, V. Werner, Y. K. Wu, and S. W. Yates *et al.*, Phys. Rev. C **70**, 044317 (2004).

[21] G. P. Glasgow, F. D. McDaniel, J. L. Weil, J. D. Brandenberger, and M. T. McEllistrem, Phys. Rev. C **18**, 2520 (1978).

[22] P. E. Garrett, H. Lehmann, J. Jolie, C. A. McGrath, M. Yeh, W. Younes, and S. W. Yates, Phys. Rev. C **64**, 024316 (2001).

[23] B. Fazekas, T. Belgya, G. Molnár, Á. Veres, R. A. Gatenby, S. W. Yates, and T. Otsuka, Nucl. Phys. **A548**, 249 (1992) and references therein.
[24] E. Sheldon and V. C. Rogers, Comput. Phys. Commun. **6**, 99 (1973); E. Sheldon (private communication).
[25] K. B. Winterbon, Nucl. Phys. **A246**, 293 (1975).
[26] K. B. Winterbon, Atomic Energy of Canada Limited Report AECL-4829 (unpublished).
[27] R. B. Firestone, in *Table of Isotopes*, edited by V. S. Shirley, 8th ed. (Wiley Interscience, New York, 1996).
[28] E. K. Warburton, C. J. Lister, D. E. Alburger, and J. W. Olness, Phys. Rev. C **23**, 1242 (1981).
[29] W. E. Collins, A. H. Welch, J. H. Hamilton, A. V. Ramayya, and N. C. Singhal, Z. Phys. A **285**, 31 (1978).
[30] K. S. Krane and R. M. Steffen, Phys. Rev. C **2**, 724 (1970).
[31] M. E. Bunker, B. J. Dropesky, J. D. Knight, and J. W. Starner, Phys. Rev. **127**, 844 (1962).
[32] T. Borello-Lewin, H. M. A. Castro, L. B. Horodynski-Matsushigue, and O. Dietzsch, Phys. Rev. C **20**, 2101 (1979).
[33] S. S. Ipson, K. C. McLean, W. Booth, and J. G. B. Haigh, Nucl. Phys. **A253**, 189 (1975).
[34] N. Lo Iudice and Ch. Stoyanov, Phys. Rev. C **69**, 044312 (2004).
[35] N. Lo Iudice and Ch. Stoyanov, Phys. Rev. C **62**, 047302 (2000); **65**, 064304 (2002).
[36] A. E. Stuchbery, N. Benczer-Koller, G. Kumbartzki, and T. J. Mertzimekis, Phys. Rev. C **69**, 044302 (2004).
[37] V. Werner, Ph.D. thesis, University of Cologne, 2004; URN: urn:nbn:de:hbz:38-12133.
[38] D. Zwarts, Comput. Phys. Commun. **38**, 365 (1985).